Journal of chemical & engineering data

Article

pubs.acs.org/jced

High Pressure Density and Speed of Sound in Two Biodiesel Fuels

Matthieu Habrioux,[†] Samuel V. D. Freitas,[‡] João A. P. Coutinho,[‡] and Jean Luc Daridon*[,†]

[†]Laboratoire des Fluides Complexes et leurs Réservoirs, Faculté des Sciences et Techniques, UMR 5150, Université de Pau, BP 1155, 64013 Pau Cedex, France

[‡]CICECO, Chemistry Department, Universityof Aveiro, Campus de Santiago, 3810−193 Aveiro, Portugal

ABSTRACT: The knowledge of high pressure densities and speeds of sound of biodiesel fuel is crucial for the optimization of diesel engines operation, namely, for the injection process, to achieve a complete combustion. However, the experimental data for these properties are still very sparse in the literature. This work reports the densities and speeds of sound measured at pressures from atmospheric to 200 MPa and temperatures from (293.15 to 393.15) K for two biodiesel fuels (soybean and rapeseed). The density data were measured only up to 100 MPa and later extrapolated for pressures up to 200 MPa by integration of speed of sound data. An equation of state was then proposed to describe both density and speed of sound within their estimated uncertainties and used to assess the density and its derivatives.

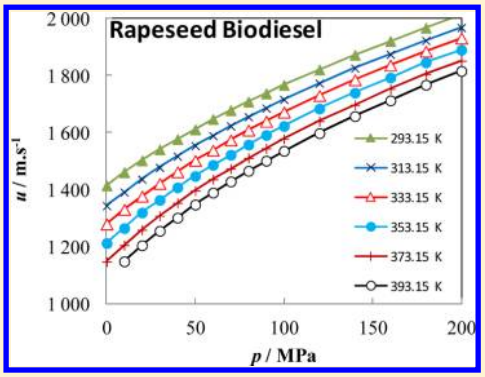

1. INTRODUCTION

The policy of reducing fuel consumption and emissions of exhaust gases forces an improvement in the performance of existing engines and the development of alternative fuels. Among possible alternative fuels, biodiesels appear as promising products as they are produced from renewable resources and are biodegradable. In the case of diesel engine working with biodiesel, one of the solutions to reduce harmful emissions consists of injecting fuel at high pressure to create a good air−fuel mixture to achieve a complete combustion.[1,2] Thus, in order to size engines and injection systems, it is necessary to know the thermo-physical properties of biodiesel in the range of pressures and temperatures of operation. Among these properties, density and isentropic compressibility have a strong influence on the injection process. These properties directly affect the amount of fuel injected into the engine cylinder through the injection system. Density is the main property that influences the conversion of volume flow rate into mass flow rate. The compressibility or bulk modulus acts on the wave amplitude but also on its velocity and thus on the fuel injection timing.[3,4] Consequently, the accurate knowledge of those proprieties of those fluids is very important for the design of the injection system.[5]

Biodiesels are produced from the transesterification of vegetable oils or animal fats with a short chain alcohol such as methanol which results in the formation of fatty acid methyl esters. Biodiesel feedstocks consist of glycerol esters of straight chain aliphatic carboxylic acids with an even number of carbon atoms ranging between 10 and 24. The chain may differ in length as well as in its degree of unsaturation. Consequently, biodiesels coming from varied sources contain esters with variable composition. This difference affects the physical properties of biodiesels and therefore the engine efficiency. Even though there are a wide variety of natural feedstocks considered for biodiesels, most of biodiesels used in North America come from soybean oils while rapeseed biodiesels are predominant in Europe. Therefore, in this paper which focuses on volumetric properties of biodiesels as a function of temperature and pressure, two biodiesels were investigated: one coming from soybean oil (biodiesel S) the other from rapeseed (biodiesel R). The work aims at characterizing the density and its derivatives by carrying out density and speed of sound measurements for temperatures ranging from (293.15 to 393.15) K in an extended range of pressure (0.1 to 100) MPa for density and (0.1 to 200) MPa for speed of sound. It follows on other investigations[6−8] of pure fatty acid methyl ester ranging from methyl caprate to methyl linoleate by the same acoustic technique.

2. EXPERIMENTAL MEASUREMENTS

2.1. Materials. The biodiesels studied in this work were synthesized by a transesterification process of two vegetable oils: soybean (supplied by Bunge Ibérica Portugal), rapeseed (supplied by Sovena) with methanol (Sigma, mole fraction purity 0.999). The molar ratio between natural feedstock oil and methanol was fixed at 1 to 5 for both oils. Sodium hydroxide was added with a weight content of 0.5 % to work as catalyst. The reaction was carried out at 328.15 K for 24 h under methanol reflux to guarantee a complete reaction conversion. After this reaction time, glycerol produced by the reaction was removed and fatty acid methyl esters that remained were purified by washing them with hot distillated water until a neutral pH was achieved. The biodiesel was then dried, and water content was checked by Karl−Fischer titration until the limit of less than 0.05 % of water was reached. Finally, the composition in methyl ester in biodiesel samples was fully identified by gas chromatography (Table 1).

Received: June 28, 2013
Accepted: October 8, 2013

   dx.doi.org/10.1021/je4006129 | J. Chem. Eng. Data XXXX, XXX, XXX−XXX

Table 1. Compositions of the Biodiesels Studied, in Mass Percentage

components	mass % soybean (S)	mass % rapeseed (R)
MeC 10:0	0	0.01
MeC 12:0	0	0.04
MeC 14:0	0.07	0.07
MeC 16:0	10.76	5.22
MeC 16:1	0.07	0.20
MeC 18:0	3.94	1.62
MeC 18:1	22.96	62.11
MeC 18:2	53.53	21.07
MeC 18:3	7.02	6.95
MeC 20:0	0.38	0.60
MeC 20:1	0.23	1.35
MeC 22:0	0.80	0.35
MeC 22:1	0.24	0.19
MeC 24:0	0	0.22

A Varian CP-3800 with a FID in a split injection system working with a Agilent column (select biodiesel for FAME 0.32 mm × 30 m × 0.25 μm) was used to discriminate between all methyl esters in analysis, including the polyunsaturated ones.

2.2. Speed of Sound. The method used to perform measurements of speed of sound at high pressure is based on a pulse echo technique working at 3 MH_Z with a path length fixed to L_0 = 30 mm. This length constitutes an acceptable compromise between shorter distances that reduce measuring accuracy and longer that increase the damping of the wave. The frequency of 3 MHz is low enough to avoid dispersion phenomena and is also a good compromise between lower frequencies (that give clear signal but with a lower precision) and higher frequencies (that give more damping of wave into the fluid but with a better precision). The apparatus, which has been described previously in detail,[6] is essentially made up of an acoustic sensor composed of two piezoelectric disks (12 mm in diameter) facing each other at both ends of a stainless steel cylindrical support. One of them generates the ultrasonic wave that travels into the fluid sample while the other is used to receive different echoes. The entire acoustic sensor is located within a stainless-steel high-pressure vessel closed at one end by a plug in which three electric connections were machined. These electric connections allow connecting both piezoelectric elements to a high voltage ultrasonic pulser−receiver device (high-voltage pulse generator (Panametrics model 5055PR). The speed of sound is determined from the measurement of the time between two successive echoes by using the base time of an oscilloscope (Tektronix TDS 1022B).[9] The path length needed for calculating speed of sound was determined at different temperatures and pressures by measuring the time-of-flight of the wave into a liquid of known speed of sound. Water[10,11] and heptane[12] were used for this calibration. This calibration leads to an uncertainty in the speed of sound of about 0.06 %.

However, the ultimate error in speed of sound measurement depends in addition on the thermal stability as well as on the uncertainty in the measurement of both temperature and pressure. To ensure a satisfactory thermal stability, the full cell is immersed in a thermostatted bath (HUBER CC410) filled with silicone oil and the temperature is directly measured into the fluid by a platinum probe (Pt100, 1.2 mm diameter) housed in a metal finger. With this configuration, temperature uncertainty leads to an additional error of 0.04 % in speed of sound. According to the pressure range investigated, two identical manometers (Hotting Baldwin Messtechnik MVD 2510) were used to measure the pressure. One is calibrated in the full pressure scale (with an uncertainty of 0.2 MPa) whereas the other is only calibrated up to 100 MPa in order to achieve a better accuracy in this range (0.02 MPa). These pressure sensors involve an error in speed of sound less than 0.1 % up to 100 MPa and 0.2 % between (100 and 200) MPa. Consequently the overall experimental uncertainty in the reported speed of sound values is estimated to be 0.2 % between (0.1013 and 100) MPa and 0.3 % between (100 and 200) MPa.

2.3. Density. Density of biodiesels was measured by a densimeter ANTON-PAAR mPDS 2000 V3 connected to a high pressure volumetric pump working up to 100 MPa. The principle of this apparatus is to measure the period of oscillation of a U-shape tube and to deduce the density which is related to the square of the period by a linear law. Vacuum and a liquid of reference were used to determine the parameters of this linear function. According to the calibration method proposed by Comuñas et al.,[13] water[14] and decane[15] were considered as reference depending on the P,T domain investigated. The temperature of the densimeter is controlled by an external circulating fluid using a thermostatic bath (Huber Ministat 125) and is measured with a Pt100 with an uncertainty of ± 0.1 K in the temperature range investigated. The pressure is transmitted to the cell by the liquid itself using a volumetric pump and measured with a HBM pressure gauge (with an uncertainty of 0.2 MPa) fixed on the circuit linking the pump to the U-tube cell. Taking into account the uncertainty of the temperature, the pressure, the density of the reference fluid as well as the error in the measurements of the period of oscillation for the vacuum and for both the reference and the studied liquid, the overall experimental uncertainty in the reported density values is estimated to be ± 0.5 kg·m^{-3} (0.06 %).

3. RESULTS AND DISCUSSION

3.1. Speed of Sound. Speed of sound measurements were carried out along isotherms spaced at 20 K interval from (293.15 to 393.15) K in the pressure range from (0.1 to 200) MPa using 10 MPa steps up to 100 MPa and 20 MPa steps beyond. Under atmospheric conditions, high temperature measurements were limited to 373.15 K due to vaporization at higher temperatures. Finally, at lower temperatures, measurements in soybean biodiesels were limited by the appearance of solid at pressures higher than 140 MPa. The data are listed in Table 2. As can be observed in Figure 1, the change of sound speed with pressure can be assumed linear between atmospheric pressure and 50 MPa with a deviation to linear behavior that for both biodiesels do not exceed 0.2 % in average in this pressure range whatever the isotherm. Real behavior deviates strongly from linearity as pressure increases beyond 50 MPa. The full set of data was fitted to a two-dimensional rational function which correlates $1/u^2$ instead of the speed of sound u:

$$\frac{1}{u^2} = \frac{A + B_1T + B_2T^2 + B_3T^3 + C_1p + C_2p^2 + C_3p^3}{1 + ET + Fp} \quad (1)$$

As the uncertainty in measurement is higher between (100 and 200) MPa than below 100 MPa, the parameters were evaluated by a least-squares weighted by the inverse square of the uncertainty. The parameters obtained in this way are listed in Table 3 along with the average deviation (AD%), the average absolute deviation (AAD%) and the maximum deviation (MD%) for both biodiesels. Observation of these deviations reveals that the correlation leads to a good interpolation of the speed of

dx.doi.org/10.1021/je4006129 | J. Chem. Eng. Data XXXX, XXX, XXX−XXX

Table 2. Experimental Values of Speed of Sound u at Temperatures T and Pressures p for Both Biodiesels S and R[a]

p	T	u	T	u	T	u
MPa	K	m·s^{-1}	K	m·s^{-1}	K	m·s^{-1}
			Biodiesel S			
0.1013	293.15	1414.9	313.15	1342.4	333.15	1276.2
10	293.15	1458.7	313.15	1388.7	333.15	1326.3
20	293.15	1499.4	313.15	1433.6	333.15	1373.9
30	293.15	1539.2	313.15	1474.6	333.15	1417.1
40	293.15	1576.1	313.15	1514.1	333.15	1459.6
50	293.15	1611.5	313.15	1550.9	333.15	1498.4
60	293.15	1643.9	313.15	1586.2	333.15	1535.2
70	293.15	1677.5	313.15	1620.0	333.15	1570.1
80	293.15	1706.9	313.15	1652.5	333.15	1604.2
90	293.15	1737.5	313.15	1683.3	333.15	1635.7
100	293.15	1766.6	313.15	1713.4	333.15	1667.3
120	293.15	1820.8	313.15	1769.0	333.15	1726.2
140	293.15	1873.8	313.15	1822.9	333.15	1781.5
160			313.15	1872.9	333.15	1831.7
180			313.15	1920.9	333.15	1881.5
200			313.15	1965.5	333.15	1927.5
0.1013	353.15	1208.8	373.15	1148.0		
10	353.15	1263.0	373.15	1200.4	393.15	1145.8
20	353.15	1314.3	373.15	1255.0	393.15	1201.8
30	353.15	1360.1	373.15	1304.0	393.15	1251.7
40	353.15	1403.6	373.15	1349.9	393.15	1299.3
50	353.15	1444.1	373.15	1392.7	393.15	1343.6
60	353.15	1482.9	373.15	1432.3	393.15	1384.9
70	353.15	1518.2	373.15	1470.4	393.15	1424.7
80	353.15	1553.9	373.15	1506.4	393.15	1462.2
90	353.15	1586.6	373.15	1540.2	393.15	1497.0
100	353.15	1618.6	373.15	1573.6	393.15	1530.7
120	353.15	1679.3	373.15	1634.1	393.15	1594.8
140	353.15	1735.7	373.15	1692.6	393.15	1652.9
160	353.15	1788.1	373.15	1746.2	393.15	1709.6
180	353.15	1838.5	373.15	1798.8	393.15	1762.2
200	353.15	1886.6	373.15	1847.9	393.15	1811.1

p	T	u	T	u	T	u
MPa	K	m·s^{-1}	K	m·s^{-1}	K	m·s^{-1}
			Biodiesel R			
0.1013	293.15	1414.2	313.15	1343.2	333.15	1279.1
10	293.15	1460.8	313.15	1391.2	333.15	1330.6
20	293.15	1502.4	313.15	1436.2	333.15	1376.8
30	293.15	1541.2	313.15	1477.4	333.15	1421.3
40	293.15	1577.1	313.15	1516.7	333.15	1462.4
50	293.15	1611.3	313.15	1553.9	333.15	1502.0
60	293.15	1647.2	313.15	1589.0	333.15	1538.1
70	293.15	1678.5	313.15	1622.9	333.15	1573.9
80	293.15	1708.6	313.15	1655.1	333.15	1608.5
90	293.15	1737.2	313.15	1685.7	333.15	1639.5
100	293.15	1766.8	313.15	1715.9	333.15	1671.6
120	293.15	1821.1	313.15	1772.9	333.15	1729.7
140	293.15	1872.4	313.15	1825.7	333.15	1785.0
160	293.15	1921.1	313.15	1874.2	333.15	1836.5
180	293.15	1967.5	313.15	1922.8	333.15	1885.3
200	293.15	2012.8	313.15	1968.3	333.15	1931.6
0.1013	353.15	1212.6	373.15	1147.7		
10	353.15	1264.9	373.15	1205.4	393.15	1148.5
20	353.15	1319.5	373.15	1259.1	393.15	1204.8
30	353.15	1363.6	373.15	1308.4	393.15	1255.5
40	353.15	1407.6	373.15	1353.4	393.15	1301.4
50	353.15	1447.7	373.15	1396.5	393.15	1347.5
60	353.15	1486.6	373.15	1436.1	393.15	1389.4
70	353.15	1522.0	373.15	1473.7	393.15	1428.5
80	353.15	1558.0	373.15	1510.9	393.15	1465.9
90	353.15	1591.3	373.15	1544.8	393.15	1501.3
100	353.15	1622.9	373.15	1578.1	393.15	1535.8
120	353.15	1684.2	373.15	1639.8	393.15	1597.9
140	353.15	1739.7	373.15	1697.1	393.15	1657.6
160	353.15	1792.8	373.15	1753.0	393.15	1712.7
180	353.15	1845.9	373.15	1804.6	393.15	1767.5
200	353.15	1890.2	373.15	1851.6	393.15	1815.9

[a]Standard uncertainties u are $u(T)$ = 0.1 K, $u(p)$ = 0.01 MPa up to 100 MPa, $u(p)$ = 0.1 MPa between (100 and 200) MPa and the combined expanded uncertainties U_c (level of confidence = 0.95) are $U_c(u)$ = 0.002 c up to 100 MPa, $U_c(u)$ = 0.003 c between (100 and 200).

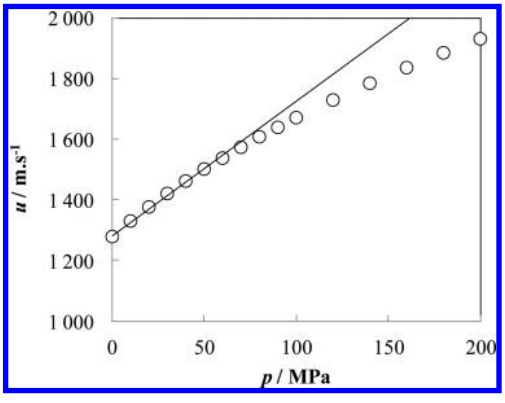

Figure 1. Speed of sound in biodiesel R as a function of pressure along isotherm 333.15 K and comparison with linear behavior.

Table 3. Parameters of eqs 1 to 3 for for Both Biodiesels S and R from (293.15 to 393.15) K and for (0.1013 to 200) MPa

parameters	biodiesel S	biodiesel R
A	$1.32041 \cdot 10^{-07}$	$1.86895 \cdot 10^{-07}$
B_1	$1.73903 \cdot 10^{-10}$	$-2.25660 \cdot 10^{-10}$
B_2	$1.60321 \cdot 10^{-12}$	$2.51521 \cdot 10^{-12}$
B_3	$-2.29230 \cdot 10^{-15}$	$-2.81390 \cdot 10^{-15}$
C_1	$1.05317 \cdot 10^{-09}$	$1.22545 \cdot 10^{-09}$
C_2	$-2.50210 \cdot 10^{-12}$	$-3.14660 \cdot 10^{-12}$
C_3	$4.01399 \cdot 10^{-15}$	$5.25238 \cdot 10^{-15}$
E	$-1.62091 \cdot 10^{-03}$	$-1.59768 \cdot 10^{-03}$
F	$5.58990 \cdot 10^{-03}$	$5.99772 \cdot 10^{-03}$
deviations[a]		
AD %	$4.6 \cdot 10^{-04}$	$3.8 \cdot 10^{-03}$
AAD %	$6.3 \cdot 10^{-02}$	$7.1 \cdot 10^{-02}$
MD %	$2.7 \cdot 10^{-01}$	$2.4 \cdot 10^{-01}$

[a]Notation: AD, average deviation; AAD, absolute average deviation; MD, maximum deviation.

sound data of both biodiesel within a maximum deviation between calculated and experimental data always inferior to the estimated experimental uncertainty. Moreover, this expression leads to a simple analytical form of the integral of $1/u^2$ with respect to pressure which represents the main contribution of the change of density with pressure. The speed of sound was measured previously in these biodiesels at atmospheric pressure by Freitas et al.[16] Comparison of these previous measurements with ours shows a good agreement with a relative deviation of 0.18 % for rapeseed, and 0.19 % for soybean that does not exceed the combined uncertainty of both experimental methods.

dx.doi.org/10.1021/je4006129 | J. Chem. Eng. Data XXXX, XXX, XXX−XXX

Table 4. .Values of Densities ρ at Temperatures T and Pressures p Measured in Liquid Biodiesels S and R by Using U-Tube Densimeter[a]

p	T	ρ	T	ρ	T	ρ	T	ρ	T	ρ	T	ρ
MPa	K	kg·m^{-3}	K	kg·m^{-3}	K	kg·m^{-3}	K	kg·m^{-3}	K	kg·m^{-3}	K	kg·m^{-3}
						Biodiesel S						
0.1013	293.15	884.9	303.15	877.6	313.15	870.5	323.15	863.1	333.15	855.8	343.15	848.6
10	293.15	890.9	303.15	883.7	313.15	876.5	323.15	869.4	333.15	862.9	343.15	855.8
20	293.15	896.2	303.15	889.6	313.15	882.6	323.15	875.6	333.15	869.2	343.15	862.4
30	293.15	901.4	303.15	895.1	313.15	888.0	323.15	881.4	333.15	875.1	343.15	868.8
40	293.15	906.7	303.15	899.7	313.15	893.4	323.15	886.5	333.15	880.9	343.15	874.4
50	293.15	910.8	303.15	904.5	313.15	898.1	323.15	892.1	333.15	886.3	343.15	879.9
60	293.15	915.0	303.15	909.3	313.15	902.7	323.15	897.2	333.15	891.5	343.15	885.3
70	293.15	919.4	303.15	913.5	313.15	907.4	323.15	902.1	333.15	896.1	343.15	890.0
80	293.15	923.7	303.15	917.9	313.15	911.8	323.15	906.2	333.15	900.8	343.15	894.7
90	293.15	927.3	303.15	922.2	313.15	915.7	323.15	910.2	333.15	905.4	343.15	899.5
100	293.15	931.3	303.15	925.7	313.15	920.3	323.15	914.5	333.15	908.9	343.15	903.9
0.1013	353.15	841.5	363.15	834.6	373.15	827.0						
10	353.15	849.2	363.15	842.1	373.15	834.9	383.15	828.2	393.15	821.1		
20	353.15	855.9	363.15	849.4	373.15	843.1	383.15	835.7	393.15	829.6		
30	353.15	862.8	363.15	856.2	373.15	849.4	383.15	843.2	393.15	837.5		
40	353.15	868.6	363.15	862.5	373.15	856.0	383.15	850.0	393.15	844.2		
50	353.15	874.5	363.15	868.2	373.15	862.3	383.15	856.2	393.15	850.7		
60	353.15	879.9	363.15	873.9	373.15	867.9	383.15	862.6	393.15	856.9		
70	353.15	885.1	363.15	879.0	373.15	873.3	383.15	867.7	393.15	862.3		
80	353.15	889.8	363.15	884.1	373.15	878.4	383.15	873.3	393.15	867.9		
90	353.15	894.7	363.15	889.3	373.15	882.9	383.15	877.7	393.15	873.2		
100	353.15	898.8	363.15	893.3	373.15	887.9	383.15	882.9	393.15	878.1		
						Biodiesel R						
0.1013	293.15	884.2	303.15	877.4	313.15	870.3	323.15	862.5	333.15	854.9	343.15	848.3
10	293.15	890.0	303.15	883.5	313.15	875.9	323.15	869.0	333.15	862.0	343.15	855.1
20	293.15	895.2	303.15	888.7	313.15	882.1	323.15	875.5	333.15	868.3	343.15	861.9
30	293.15	900.6	303.15	894.3	313.15	888.0	323.15	880.9	333.15	874.4	343.15	867.9
40	293.15	905.6	303.15	899.1	313.15	893.1	323.15	886.2	333.15	880.3	343.15	873.6
50	293.15	909.9	303.15	903.8	313.15	897.6	323.15	891.5	333.15	885.2	343.15	879.4
60	293.15	914.0	303.15	908.3	313.15	902.1	323.15	896.3	333.15	890.4	343.15	884.8
70	293.15	918.5	303.15	912.8	313.15	906.6	323.15	900.9	333.15	895.2	343.15	889.4
80	293.15	922.9	303.15	917.1	313.15	911.1	323.15	905.2	333.15	899.7	343.15	893.5
90	293.15	926.5	303.15	921.1	313.15	914.8	323.15	909.3	333.15	903.9	343.15	898.5
100	293.15	929.8	303.15	925.2	313.15	919.3	323.15	914.0	333.15	908.1	343.15	903.5
0.1013	353.15	840.7	363.15	833.3	373.15	826.0						
10	353.15	848.3	363.15	840.8	373.15	834.2	383.15	827.4	393.15	820.0		
20	353.15	854.8	363.15	848.1	373.15	841.3	383.15	834.9	393.15	828.6		
30	353.15	861.7	363.15	854.9	373.15	848.6	383.15	842.4	393.15	836.3		
40	353.15	867.6	363.15	861.1	373.15	855.2	383.15	849.0	393.15	843.0		
50	353.15	873.4	363.15	867.1	373.15	861.3	383.15	855.1	393.15	849.5		
60	353.15	878.6	363.15	872.7	373.15	866.7	383.15	861.6	393.15	855.5		
70	353.15	884.1	363.15	878.0	373.15	872.2	383.15	866.3	393.15	861.1		
80	353.15	888.8	363.15	883.1	373.15	877.5	383.15	871.5	393.15	866.6		
90	353.15	893.4	363.15	887.7	373.15	882.1	383.15	876.7	393.15	871.9		
100	353.15	897.6	363.15	892.5	373.15	886.5	383.15	881.1	393.15	876.7		

[a]Standard uncertainties u are $u(T)$ = 0.1 K, $u(p)$ = 0.01 MPa and the combined expanded uncertainties U_c (level of confidence = 0.95) is $U_c(\rho)$ = 0.5 kg·m^{-3}.

Despite the difference in composition, speed of sound measurements are very similar with a deviation between two sets of experiments that does not exceed 10 m·s^{-1} in the full p,T range investigated. Moreover, as it can be observed in Figure 2, the speed of sound values are very close to those of oleate[8] (C18:1) and linoleate[8] (C18:2) which represent the main components of the biodiesels.

3.2. Density. The density was measured by the U-tube densimeter from (293.15 and 393.15) K every 10 K and from (0.1013 to 100) MPa with a pressure step of 10 MPa. The results are given in Table 4. In addition, density determination was extended to 200 MPa by integration of speed of sound data. This method, which has been previously used to determinate the density of mercury[17] or water[18] as well as the density of several hydrocarbon liquids,[19,20] rests on the relationships between the speed of sound and the isentropic compressibility κ_s:

$$\kappa_s = \frac{1}{\rho u^2} \tag{2}$$

dx.doi.org/10.1021/je4006129 | J. Chem. Eng. Data XXXX, XXX, XXX−XXX

Table 5. Values of Densities ρ at Temperatures T and Pressures p Determined from Integration of Speed of Sound Measurements in Both Biodiesels S and R[a]

p	T	ρ	T	ρ	T	ρ	p	T	ρ	T	ρ	T	ρ
MPa	K	kg·m^{-3}	K	kg·m^{-3}	K	kg·m^{-3}	MPa	K	kg·m^{-3}	K	kg·m^{-3}	K	kg·m^{-3}
Biodiesel S							Biodiesel R						
0.1013	293.15	885.0	313.15	870.3	333.15	855.9	0.1013	293.15	884.4	313.15	869.9	333.15	855.4
10	293.15	890.8	313.15	876.6	333.15	862.8	10	293.15	890.1	313.15	876.2	333.15	862.3
20	293.15	896.3	313.15	882.5	333.15	869.2	20	293.15	895.5	313.15	882.1	333.15	868.7
30	293.15	901.5	313.15	888.1	333.15	875.2	30	293.15	900.6	313.15	887.6	333.15	874.7
40	293.15	906.4	313.15	893.3	333.15	880.8	40	293.15	905.5	313.15	892.9	333.15	880.4
50	293.15	911.1	313.15	898.3	333.15	886.2	50	293.15	910.1	313.15	897.8	333.15	885.7
60	293.15	915.6	313.15	903.1	333.15	891.2	60	293.15	914.5	313.15	902.6	333.15	890.7
70	293.15	919.9	313.15	907.6	333.15	896.0	70	293.15	918.8	313.15	907.1	333.15	895.5
80	293.15	924.1	313.15	912.0	333.15	900.6	80	293.15	922.8	313.15	911.4	333.15	900.1
90	293.15	928.1	313.15	916.2	333.15	905.0	90	293.15	926.8	313.15	915.5	333.15	904.5
100	293.15	932.0	313.15	920.2	333.15	909.2	100	293.15	930.6	313.15	919.5	333.15	908.7
120	293.15	939.4	313.15	927.9	333.15	917.2	120	293.15	937.8	313.15	927.1	333.15	916.7
140	293.15	946.3	313.15	935.1	333.15	924.7	140	293.15	944.5	313.15	934.2	333.15	924.2
160			313.15	941.9	333.15	931.7	160	293.15	950.9	313.15	940.9	333.15	931.2
180			313.15	948.3	333.15	938.4	180	293.15	957.0	313.15	947.3	333.15	937.8
200			313.15	954.5	333.15	944.7	200	293.15	962.8	313.15	953.3	333.15	944.0
0.1013	353.15	841.6	373.15	827.0			0.1013	353.15	840.7	373.15	825.9		
10	353.15	849.1	373.15	835.4	393.15	821.3	10	353.15	848.3	373.15	834.3	393.15	820.2
20	353.15	856.2	373.15	843.1	393.15	829.7	20	353.15	855.3	373.15	842.0	393.15	828.6
30	353.15	862.6	373.15	850.1	393.15	837.5	30	353.15	861.9	373.15	849.0	393.15	836.3
40	353.15	868.7	373.15	856.7	393.15	844.6	40	353.15	867.9	373.15	855.6	393.15	843.3
50	353.15	874.4	373.15	862.8	393.15	851.2	50	353.15	873.6	373.15	861.7	393.15	849.9
60	353.15	879.8	373.15	868.5	393.15	857.3	60	353.15	879.0	373.15	867.4	393.15	856.0
70	353.15	884.8	373.15	873.9	393.15	863.1	70	353.15	884.1	373.15	872.9	393.15	861.8
80	353.15	889.7	373.15	879.1	393.15	868.6	80	353.15	889.0	373.15	878.0	393.15	867.3
90	353.15	894.3	373.15	884.0	393.15	873.8	90	353.15	893.6	373.15	882.9	393.15	872.4
100	353.15	898.8	373.15	888.7	393.15	878.7	100	353.15	898.1	373.15	887.6	393.15	877.4
120	353.15	907.1	373.15	897.4	393.15	888.0	120	353.15	906.5	373.15	896.4	393.15	886.6
140	353.15	914.9	373.15	905.6	393.15	896.5	140	353.15	914.3	373.15	904.6	393.15	895.1
160	353.15	922.2	373.15	913.1	393.15	904.4	160	353.15	921.6	373.15	912.2	393.15	903.1
180	353.15	929.1	373.15	920.3	393.15	911.8	180	353.15	928.5	373.15	919.4	393.15	910.5
200	353.15	935.6	373.15	927.0	393.15	918.8	200	353.15	935.0	373.15	926.1	393.15	917.5

Standard uncertainties u are $u(T)$ = 0.1 K, $u(p)$ = 0.01 MPa up to 100 MPa, $u(p)$ = 0.1 MPa between (100 and 200) MPa and the combined expanded uncertainties U_c (level of confidence = 0.95) are $U_c(\rho)$ = 0.001 ρ up to 100 MPa and $U_c(\rho)$ = 0.002 ρ between (100 and 200) MPa.

The combination of this equation with the so call Newton−Laplace relationships

$$\kappa_T = \kappa_S + \frac{T\alpha^2}{\rho C_P} \tag{3}$$

leads to an expression of the change in density with respect to pressure:

$$\rho(p, T) = \rho(p_0, T) + \int_{p_0}^{p} \frac{1}{u^2}\, dp + T\int_{p_0}^{p} \frac{\alpha^2}{C_P}\, dp \tag{4}$$

where α_P represents the isobaric thermal expansion, c_p is the isobaric heat capacity. This last equation provides an accurate method to determine liquid density under pressure when properties are known at atmospheric pressure $\rho(p_0,T)$. The first integral which represents the most important contribution to the variation of the density with the pressure is evaluated by analytical integration of eq 1 with the fitted parameters of Table 3. The second integral, that can be regarded as perturbation of the first one, is evaluated iteratively using a predictor−corrector procedure.[21,22] The heat capacities required to initiate this iterative procedure were measured at atmospheric pressure by using a SETARAM Micro DSC 7 evo calorimeter and were expressed as a linear function of temperature in the range investigated:

$$c_{P,\mathrm{ref}}(\mathrm{S})/\mathrm{J{\cdot}K^{-1}{\cdot}kg^{-1}} = 1.184 \times 10^3 + 2.865T \tag{5}$$

$$c_{P,ref}(\mathrm{R})/\mathrm{J{\cdot}K^{-1}{\cdot}kg^{-1}} = 1.218 \times 10^3 + 2.760T \tag{6}$$

The data obtained by this method are reported in Table 5. As for speed of sound, density measurements have comparable values with pure methyl esters, especially with linoleate (Figure 3).

Simultaneous knowledge of speed of sound and density in the same conditions makes possible an evaluation of isentropic compressibility with an uncertainty of 0.5 % up to 100 MPa and 0.9 % between (100 and 210) MPa by using eq 2. Ultimately, the knowledge of both density and speed of sound allows an adjustment of the parameters of an equation of state function defined by the volume at atmospheric pressure and the change in volume with respect to pressure:

$$v(P_0, T) = v_0 + v_1T + v_2T^2 + v_3T^3 \tag{7}$$

dx.doi.org/10.1021/je4006129 | J. Chem. Eng. Data XXXX, XXX, XXX−XXX

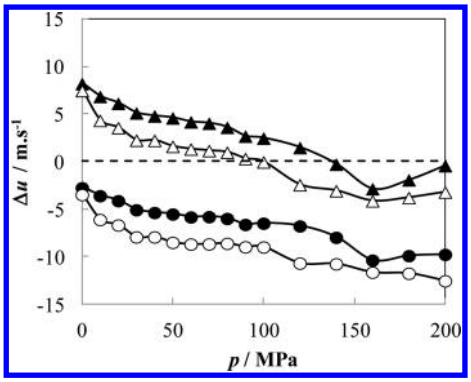

Figure 2. Deviations between speed of sound measurements in biodiesels and pure fatty acid methyl esters (C18:1 and C18:2) at 313.15 K. ▲, $\Delta u = u$(biodiesel R) − u(C18:1); ●, $\Delta u = u$(biodiesel R) − u(C18:2); △, $\Delta u = u$(biodiesel S) − u(C18:1); ○, $\Delta u = u$(biodiesel S) − u(C18:2).

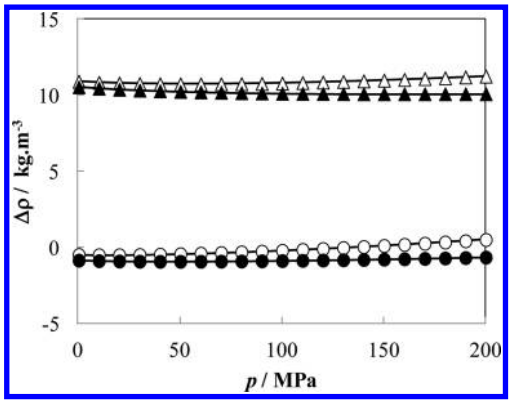

Figure 3. Deviations between density measurements in biodiesels and pure fatty acid methylesters (C18:1 and C18:2) at 313.15 K. ▲, $\Delta\rho = \rho$(biodiesel R) − ρ(C18:1); ●, $\Delta\rho = \rho$(biodiesel R) − ρ(C18:2); △: $\Delta\rho = \rho$(biodiesel S) − ρ(C18:1); ○, $\Delta\rho = \rho$(biodiesel S) − ρ(C18:2).

$$\left(\frac{\partial v}{\partial p}\right)_T = -\frac{a + cp}{b + p} \tag{8}$$

where c is constant and a and b are expressed as a function of temperature by means of polynomial functions:

$$a = a_0 + a_1 T + a_2 T^2 + a_3 T^3 \tag{9}$$

$$b = b_0 + b_1 T + b_2 T^2 \tag{10}$$

By successive integration of this equation with respect to pressure and derivation with respect to temperature, the volume and its related thermophysical properties, that is, isobaric expansion, isothermal compressibility, heat capacity, and finally isentropic compressibility and speed of sound can be calculated. All the details concerning the various stages in the calculations of these properties are detailed in a previous paper.[7] Parameters of eq 7 were first determined by a least-squares fitting of atmospheric density data. Then parameters of eqs 8 to 10 were adjusted by minimizing the following objective function:

$$\mathrm{OF} = \sum_i^{N_{\exp}} \left(-\left(\frac{\partial v}{\partial p}\right)_T^{\mathrm{cal}} - \frac{T}{c_P^{\mathrm{cal}}}\left(\frac{\partial v}{\partial T}\right)_p^{2,\mathrm{cal}} - \left(\frac{v_i^{\exp}}{u_i^{\exp}}\right)^2 \right)^2 \tag{9}$$

The values of the height coefficients determined in this way are given in Table 6 along with the average deviation, the average absolute deviation, and the maximum deviation with experimental data for both the density and the speed of sound. In the case of density, comparison with data of Pratas et al.[23] between (293.15 and 333.15) K and up to 45 MPa were also reported in Table 6. Observation of these deviations show that the function provides a very good representation of density in the range of pressure temperature investigated. By comparing the deviations obtained with both U-tube measurements and speed of sound integration, it is found that both sets of data are in good agreement within the experimental uncertainty. This result indicates the overall consistency between the speed of sound and the density measurements. Comparison with data reported by Pratas et al.[23] also shows a good agreement with a maximum deviation of 0.06 % for rapeseed and 0.17 % for soybean biodiesel. Finally, the proposed equation enables a calculation of the speed of sound up to 200 MPa with a maximum deviation less than the experimental error. Therefore the proposed equation can be used to characterize the density and its derivatives with a good reliability within the extended pressure range from (0.1013 to 200) MPa.

Table 6. Parameters of eqs 7 to 10 from (293.15 to 393.15) K and for (0.1013 to 200) MPa and Deviations from Sound Speed and Density Data

parameters	biodiesel S	biodiesel R
v_0	$6.01097 \cdot 10^{-04}$	$8.61887 \cdot 10^{-04}$
v_1	$3.41770 \cdot 10^{-06}$	$1.11902 \cdot 10^{-06}$
v_2	$-8.11710 \cdot 10^{-09}$	$-1.40900 \cdot 10^{-09}$
v_3	$8.91211 \cdot 10^{-12}$	$2.45458 \cdot 10^{-12}$
a_0	$3.56032 \cdot 10^{-05}$	$2.02269 \cdot 10^{-05}$
a_1	$6.10928 \cdot 10^{-07}$	$4.69300 \cdot 10^{-07}$
a_2	$-2.25910 \cdot 10^{-09}$	$-1.18950 \cdot 10^{-09}$
a_3	$2.82398 \cdot 10^{-12}$	$1.28740 \cdot 10^{-12}$
b_0	$4.32654 \cdot 10^{+02}$	$3.82916 \cdot 10^{+02}$
b_1	−1.45865	−1.22036
b_2	$1.32764 \cdot 10^{-03}$	$1.05019 \cdot 10^{-03}$
c	$4.38171 \cdot 10^{-08}$	$4.37953 \cdot 10^{-08}$
deviations[a]		
AD % for ρ from speed of sound	$6.1 \cdot 10^{-04}$	$1.7 \cdot 10^{-03}$
AAD % for ρ from speed of sound	$2.0 \cdot 10^{-03}$	$2.2 \cdot 10^{-03}$
MD % for ρ from speed of sound	$6.6 \cdot 10^{-03}$	$7.8 \cdot 10^{-03}$
AD % for ρ U-tube	$2.5 \cdot 10^{-02}$	$3.9 \cdot 10^{-02}$
AAD % for ρ U-tube	$3.5 \cdot 10^{-02}$	$4.4 \cdot 10^{-02}$
MD % for ρ U-tube	$1.3 \cdot 10^{-01}$	$1.6 \cdot 10^{-01}$
AD % for ρ Pratas et al.[23]	$-1.3 \cdot 10^{-01}$	$1.8 \cdot 10^{-02}$
AAD % for ρ Pratas et al.[23]	$1.3 \cdot 10^{-01}$	$2.2 \cdot 10^{-02}$
MD % for ρ Pratas et al.[23]	$1.7 \cdot 10^{-01}$	$7.3 \cdot 10^{-02}$
AD % for u	$4.6 \cdot 10^{-03}$	$-7.2 \cdot 10^{-03}$
AAD % for u	$8.0 \cdot 10^{-02}$	$8.9 \cdot 10^{-02}$
MD % for u	$4.8 \cdot 10^{-01}$	$2.5 \cdot 10^{-01}$

[a]Notation: AD, average deviation; AAD, absolute average deviation; MD, maximum deviation.

4. CONCLUSIONS

Speed of sound measurements were carried out in an extended range of pressure in biodiesels coming from the transesterification of a soybean and a rapeseed oil with methanol. Densities were measured in the same biodiesels by using a U-tube densimeter up to 100 MPa and were determined between atmospheric pressure and 200 MPa by integration of the speed of sound data. The measurements were used to determine isentropic and isothermal compressibilities in the same P,T conditions than speed of sound measurements.

dx.doi.org/10.1021/je4006129 | J. Chem. Eng. Data XXXX, XXX, XXX−XXX

AUTHOR INFORMATION

Corresponding Author

*E-mail: jean-luc.daridon@univ-pau.fr.

Funding

Samuel Freitas acknowledges a Ph.D. Grant from Fundação para a Ciência e a Tecnologia through his Ph.D. Grant SFRH/BD/51476/2011, Fundação Oriente, and also financial support from the University of Aveiro. CICECO is being funded by Fundação para a Ciência e a Tecnologia through Pest-C/CTM/LA0011/2011.

Notes

The authors declare no competing financial interest.

REFERENCES

(1) Wang, X.; Huang, Z.; Zhang, W.; Kuti, O.; Nishida, K. Effects of ultra-high injection pressure and micro-hole nozzle on flame structure and soot formation of impinging diesel spray. *Appl. Energy* **2011**, *88*, 1620−1628.

(2) Celıkten, I. An experimental investigation of the effect of the injection pressure on engine performance and exhaust emission in indirect injection diesel engines. *Appl. Therm. Eng.* **2003**, *23*, 2051−2060.

(3) Boudy, F.; Seers, P. Impact of physical properties of biodiesel on the injection process in a common-rail direct injection system. *Energy Convers. Manage.* **2009**, *50*, 2905−2912.

(4) Boehman, A. L.; Morris, D.; Szybist, J. The impact of the bulk modulus of diesel fuels on fuel injection timing. *Energy Fuels* **2004**, *18*, 1877−1882.

(5) Lapuerta, M.; Agudelo, J. R.; Prorok, M.; Boehman, A. L. Bulk modulus of compressibility of diesel/biodiesel/HVO blends. *Energy Fuels* **2012**, *26*, 1336−1343.

(6) Ndiaye, E. H. I.; Nasri, D.; Daridon, J. L. Speed of sound, density, and derivative properties of fatty acid methyl and ethyl esters under high pressure: Methyl caprate and ethyl caprate. *J. Chem. Eng. Data* **2012**, *57*, 2667−2676.

(7) Ndiaye, E. H. I.; Habrioux, M.; Coutinho, J. A. P.; Paredes, M. L. L.; Daridon, J. L. Speed of sound, density, and derivative properties of ethyl myristate, methyl myristate, and methyl palmitate under high pressure. *J. Chem. Eng. Data* **2013**, *58*, 1371−1377.

(8) Ndiaye, E. H. I.; Habrioux, M.; Coutinho, J. A. P.; Paredes, M. L. L.; Nasri, D.; Daridon, J. L. Speed of sound, density and derivative properties of methyl oleate and methyl linoleate under high pressure. *J. Chem. Eng. Data* **2013**, *58*, 2345−2354.

(9) Dutour, S.; Daridon, J. L.; Lagourette, B. Pressure and temperature dependence of the speed of sound and related properties in normal octadecane and nonadecane. *Int. J. Thermophys.* **2000**, *21*, 173−184.

(10) Wilson, W. D. Speed of sound in distilled water as a function of temperature and pressure. *J. Acoust. Soc. Am.* **1959**, *31*, 1067−1072.

(11) Baltasar, E. H.; Taravillo, M.; Baonza, V. G.; Sanz, P. D.; Guignon, B. Speed of sound in liquid water from (253.15 to 348.15) K and pressures from (0.1 to 700) MPa. *J. Chem. Eng. Data* **2011**, *56*, 4800−4807.

(12) Daridon, J. L.; Lagrabette, A.; Lagourette, B. Speed of sound, density, and compressibilities of heavy synthetic cuts from ultrasonic measurements under pressure. *J. Chem. Thermodyn.* **1998**, *30*, 607−623.

(13) Comuñas, M. J. P.; Bazil, J. P.; Baylaucq, A.; Boned, C. Density of diethyl adipate using a vibrating densimeter from 293.15 to 403.15 K and up to 140 MPa. densimeter calibration and measurements. *J. Chem. Eng. Data* **2008**, *53*, 986−994.

(14) Wagner, W.; Pruß, A. The IAPWS formulation 1995 for the thermodynamic properties of ordinary water substance for general and scientific use. *J. Phys. Chem. Ref. Data* **2002**, *31*, 387−535.

(15) TRC. *Thermodynamic Tables*; Texas A&M University, College Station: TX, 1996.

(16) Freitas, S. V. D.; Paredes, M. L. L.; Daridon, J.-L.; Lima, Á. S.; Coutinho, J. A. P. Measurement and prediction of the speed of sound of biodiesel fuels. *Fuel* **2013**, *103*, 1018−1022.

(17) Davis, L. A.; Gordon, R. B. Compression of mercury at high pressure. *J. Chem. Phys.* **1967**, *46*, 2650−2660.

(18) Kell, G. S.; Whalley, E. Reanalysis of the density of liquid water in the range 0−150 °C and 0−1 kbar. *J. Chem. Phys.* **1975**, *62*, 3496−3503.

(19) Muringer, M. J. P.; Trappeniers, N. J.; Biswas, S. N. The effect of pressure on the sound-velocity and density of toluene and *n*-heptane up to 2600 bar. *Phys. Chem. Liq.* **1985**, *14*, 273−295.

(20) Sun, T. F.; Schouten, J. A.; Biswas, S. N. Determination of the thermodynamic properties of liquid ethanol from 193 to 263 K and up to 280 MPa from speed-of-sound measurements. *Int. J. Thermophys.* **1991**, *12*, 381−395.

(21) Daridon, J. L.; Lagourette, B.; Grolier, J. P. Measure and exploitation of ultrasonic speed in *n*-hexane up to 150 MPa. *Int. J. Thermophys.* **1998**, *19*, 145−160.

(22) Daridon, J. L.; Lagourette, B.; Lagrabette, A. Acoustic determination of thermodynamic properties of ternary mixtures up to 150 MPa. *Phys. Chem. Liq.* **1999**, *37*, 137−160.

(23) Pratas, M. J.; Oliveira, M. B.; Pastoriza-Gallego, M. J.; Queimada, A. J.; Pieiro, M. M.; Coutinho, J. A. P. High-pressure biodiesel density: Experimental measurements, correlation, and cubic-plus-association equation of state (CPA EoS) modeling. *Energy Fuels* **2011**, *25*, 3806−3814.